Preprints of the 21st IFAC World Congress (Virtual)
Berlin, Germany, July 12-17, 2020

Discrete Reduced-order Active Disturbance Rejection Control for Marine engines using Variable Sampling Rate Control Scheme under Limited Bandwidth

Runzhi Wang, Xuemin Li*, Xiuzhen Ma

College of Power and Energy Engineering, Harbin Engineering University, Harbin, China 150001
(Tel: +86-8251-9249; e-mail: wangrunzhiyuqing@foxmail.com, lxm@hrbeu.edu.cn, maxiuzhen@hrbeu.edu.cn).

Abstract: In this paper, the reduced-order active disturbance rejection control (RADRC) is studied for marine engine speed control. The benefits of using RADRC are demonstrated by bode diagram method with the transfer function between input disturbance and system output. Discrete RADRC and active disturbance rejection control (ADRC) are designed for marine engine speed control by adopting variable sampling rate control method. The proposed method is assessed by experiment on a hard-in-loop (HIL) engine test platform. Except the step-response indexes, ADRC and RADRC are compared in more indexes. The results demonstrate that RADRC has superiority during the sudden load varying process. For steady-state, a single smaller observer bandwidth in RADRC can make a good compromise for a wide range engine speed. It also has been found that the index of total variation (TV) in control input for RADRC is inferior to the ADRC. Overall, RADRC is a promising method for marine engine speed control.

Keywords: Active disturbance rejection control, marine diesel engine, speed control, variable sampling rate control.

1. INTRODUCTION

Diesel engines are widely used in the domain of ship propulsion. Under such condition, the engine speed regulation becomes a crucial task. First, the speed control of the engine affects the safety of the ship, a good speed controller can provide safer marine navigation for ships. Second, the lifetime of the ship and marine main engine is directly related to the operation of the marine main engine, because the vibration of the propulsion system is often triggered by undesired speed fluctuation of the marine main engine.

The primary difficulties for marine engine speed control are original from two sides, i.e., 1) the inherent uncertainties and nonlinearities of the engine system; 2) the unpredictable external maritime environment (mainly affects the load condition). Extensive works have been focused on the marine engine speed control. For instance, model predictive control (MPC) has been investigated under safety and emission constraints to regulate the speed of the diesel generators used onboard submarines (Broomhead et al., 2017). In (Papalambrou and Kyrtatos, 2006), H_∞ control method is tested for marine engine speed control by using a set of linearized engine models. Sliding model control (SMC) is studied in (Li et al., 2017) and (Yuan et al., 2018) for diesel engines applied in ship propulsion. However, the simplest PID controllers are still the mainstream commercially employed ones in the marine engine speed control due to the higher hardware requirements and more complex tuning parameters of the new emerged control algorithms. When PID controller is used in marine engine speed control, troublesome parameters calibration should be considered. Yet despite all that, when the operating condition of the marine engine deviates far away from its calibrated condition, the marine engine always suffers from the poor performance in engine speed regulation. It is still a big challenge to design a sufficient robust controller for marine engine speed control in the presence of uncertainty and disturbance. Recently, active disturbance rejection control (ADRC) known as a promising algorithm that can replace the general PID has been explored in marine engine speed control. In (Weigang et al., 2010) a continuous nonlinear active disturbance rejection speed controller is designed for marine main engine and verified on a simplified transfer function engine model. Later, a compound discrete linear-nonlinear ADRC scheme is analysed for marine engine speed regulation in (Wang et al., 2018a), the authors find that nonlinear extended state observer (ESO) cannot provide a satisfactory estimation and compensation when the total disturbance is large. In (Wang et al., 2019b), to consider the event-based traits in practical engine speed controller, a variable sampling rate control based linear ADRC is designed. The results show that the linear ADRC with variable sampling control technique can meet the event-based control scheme in practical engine speed controller, meanwhile, can improve the speed control performance, especially, under the external load variation.

On the basis of the research in (Wang et al., 2019b) mentioned above, in this study, we will consider how to further improve the control performance of the proposed variable sampling rate based ADRC. To improve the control performance of the ADRC, various works have been drawn on how to modified the existed ESO or ADRC. In (Tatsumi et al., 2013), the methods concerning improving the control effect of ADRC under limited bandwidth is analysed systemically, including the most practical and easiest way that is via using the real state

variables to replace the estimated states in control law. In Ref (Huang and Xue, 2014, Yang et al., 2011, Chen et al., 2019), the reduced-order ESO (RESO) is studied under the condition when system state can be measured directly. It has been proved that the RESO can estimate and compensate the total disturbance faster than the general ESO and thus improve the control performance (Shao and Wang, 2015). However, in engine speed control domain, from the published works, the ADRC is still based on the general ESO. Hence, it is meaningful to investigate the control effect of the RESO based ADRC in engine speed control. This is the primary purpose of this study. In addition, to give the reason why RESO has better control performance than the general ESO, the transfer function between the disturbance and its estimated disturbance in ESO/RESO is analysed with bode diagram method in (Shao and Wang, 2015). However, in this study, more intuitively, the frequency domain analysis of the transfer function between disturbance and the measured system output is provided.

The rest of the paper is organized as follows. In section 2, the description of engine speed control model is given. Section 3 shows the design of reduced-order ADRC (RADRC) using variable sampling control technique. And the frequency domain analysis of the ADRC and RADRC is given. The comparison is demonstrated in section 4. A conclusion is provided in section 5.

2. CYLINDER-BY-CYLINDER MEAN VALUE ENGINE MODEL

As discussed in (Wang et al., 2018b, Wang et al., 2018a, Wang et al., 2019b), the common mean value engine model (MVEM) cannot simulate the inherent engine fluctuation during the working cycle caused by the discrete torque generation in internal combustion engines. On the basis of the authors' previous works (Wang et al., 2018b), the cylinder-by-cylinder MVEM is introduced briefly in this section. In such engine model, the crank-angle (CA) signal can be given as follow

$$\varphi = mod\left(\int \frac{\pi n_e}{30} dt, 4\pi\right), \tag{1}$$

where n_e is engine speed on crankshaft, 'mod' means the modulus operator.

With the CA signal φ, for individual cylinder i, the discrete indicated torque generation can be given as

$$M_{ig}^i = \emptyset_d \frac{120 \cdot W_f^i \cdot q_{HV} \cdot \eta_{ind}^i \xi_i}{n_e N_{cyl} \cdot \varphi_F}, \tag{2}$$

$$\eta_{ind} = g(n_e, \lambda), \tag{3}$$

with

$$\emptyset_d = \begin{cases} 1 \ (i-1)\dfrac{2\pi}{N_{cyl}} < \varphi < (i-1)\dfrac{2\pi}{N_{cyl}} + \varphi_F \\ 0 \qquad otherwise \end{cases}, \tag{4}$$

where $i = 1,2,\dots,N_{cyl}$, M_{ig}^i is the indicated torque of cylinder i, φ_F is the firing duration (for 4-stroke engine, it is set to be π rad), $\emptyset_d$ is a block pulse function to represent the discrete torque generation in engines. W_f^i and η_{ind}^i denote the fuel mass flow rate and the indicated efficiency of the cylinder i, ξ_i is the unevenness of the cylinder i about its powering ability.

As a result, the total indicated torque for all the cylinders is

$$M_{ig} = \sum\nolimits_1^{N_{cyl}} M_{ig}^i, \tag{5}$$

The engine speed dynamic on the crankshaft can be given as

$$\frac{d}{dt} n_e = \frac{30}{\pi J_e}\left(M_{ig} - M_{total}\right), \tag{6}$$

where J_e is the total rotational inertia, M_{total} is the total load disturbance including the pump losing torque M_p, the friction torque M_f, the external load torque M_l, etc.

Remark 1. The indicated torque M_{ig} is a high nonlinear function of engine speed and indicated efficiency, the total load disturbance torque also has a complex relationship with the engine speed. Besides, the external condition, e.g., the maritime, has a huge influence on the engine operation condition. Those factors make the engine speed control a complex issue with strong nonlinearity and extensive uncertainty.

3. CONTROLLER DESIGN

3.1 Frequency domain analysis of the general ADRC and RADRC

As explained above, if ignore the time delay, the diesel engine speed control model is first-order, whose transfer model can be written as

$$P(s) = \frac{K}{Ts + 1}, \tag{7}$$

where $P(s)$ is the transfer function between control input W_f^i and system output n_e, K and T are the system gain and time constant, respectively.

Note that this kind of model is valid only around a certain engine speed with a certain load condition. More detailed information about the simplification of engine speed control model can refer to (Jammoussi et al., 2014, Memering and Meckl, 2002, Wang et al., 2018b).

If consider external disturbance d, the state space expression of system (7) is

$$\begin{cases} \dot{x}_1 = f + b_0 u \\ y = x_1 \end{cases}, \tag{8}$$

where b_0 is an estimated gain towards control input u, $f = \left(\frac{K}{T} - b_0\right)u + d$ is regarded as the total disturbance.

Assuming f is differentiable, given the extended state $x_2 = f$, system (8) can be rewritten as

$$\begin{cases} \dot{x}_1 = x_2 + b_0 u \\ \dot{x}_2 = \dot{f} \\ y = x_1 \end{cases}. \tag{9}$$

The general ADRC for system (7) can be given as follow

$$\text{ESO: } \begin{cases} \dot{z}_1 = z_2 + b_0 u + 2\omega_o (y - z_1) \\ \dot{z}_2 = {\omega_o}^2 (y - z_1) \end{cases}, \tag{10}$$

$$\text{Control law: } u = \frac{k_p (r - z_1) - z_2}{b_0}, \tag{11}$$

where r is the reference signal, z_1, z_2 are the estimation of system output y and total disturbance f, k_p is control bandwidth, ω_o is the observer bandwidth. More details about the parameters design for ADRC can refer to (Gao, 2003).

It has been found that using the measured system output y in control law can improve the performance of ADRC, hence, replacing z_1 with y in control law (11), we can get a controller defined to be "ADRC-y". For the original ADRC, it can be defined as "ADRC-z1".

Various works regarding the application of ADRC have been focused on improving the control performance by employing RESO (Chen et al., 2019, Yang et al., 2011). The observer bandwidth in the RESO can be reduced largely. According to (Yang et al., 2011), the RADRC can be given as

$$\text{RESO: } \begin{cases} \dot{v} = -\omega_o(b_0 u + (v + \omega_o x_1)) \\ z_2 = v + l x_1 \end{cases}, \tag{12}$$

$$\text{Control law: } u = \frac{k_p(r-y)-z_2}{b_0}, \tag{13}$$

where v is an intermediate variable.

According to (Yang et al., 2011), for system (7), ADRC-y and RADRC can be shown in Fig. 1 (b) and (c), respectively. Similarly, ADRC-z1 can be given in Fig. 1 (a). We consider the inner loop that copes with the equivalent input disturbance directly. For ADRC-z1, ADRC-y, and RADRC, their inner loop transfer functions from equivalent input disturbance *D(s)* to system output *Y(s)* are given in Table 1. Given parameters K=10, T=2 for the system (7), first, we design parameters for the mentioned three controllers to guarantee their step-response being monotone nondecreasing without overshoot under two different observer bandwidths. Table 2 shows the detailed values for control parameters. The rules are borrowed from (Yang et al., 2011).

Figure 2 shows that the step-response of the three compared controllers under parameters set 1 and 2. For the three controllers, they all have similar performance during the step-response. However, when a step disturbance is added in at 10s, the overshoot in RADRC is significantly smaller than others.

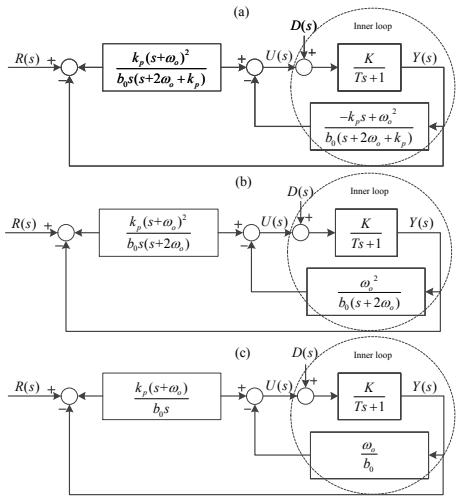

Fig. 1 The equivalent block diagrams

To understand this better, in Fig. 3, we give the bode diagrams of the inner loop transfer function for these controllers with different observer bandwidths. It is apparently that ADRC-z1 and ADRC-y have poor performance under low observer bandwidth ($\omega_o = 10$). The disturbance cannot be attenuated by inner loop in ADRC-z1 and ADRC-y under low bandwidth, resulting in more burden for external loop to deal with the disturbance. On the contrary, inner loop of RADRC keeps a considerable attenuation of the disturbance under the low observer bandwidth. When observer bandwidth is high, all three of them can reduce the amplitude of disturbance in the low frequency region, but ADRC-z1 has more phase loss.

Table 1. The Equivalent Inner Loop Transfer Functions

Controller	Inner loop transfer function $(Y(s)/D(s))$
ADRC-z1	$\frac{Kb_0(s+2\omega_0+k_p)}{b_0Ts^2+[b_0(2\omega_oT+k_pT+1)-Kk_p]s+2\omega_ob_0+k_pb_0+K\omega_o^2}$
ADRC-y	$\frac{Kb_0(s+2\omega_o)}{b_0Ts^2+(2\omega_oT+1)b_0s+2\omega_ob_0+K\omega_o^2}$
RADRC	$\frac{Kb_0}{b_0Ts+b_0+K\omega_0}$

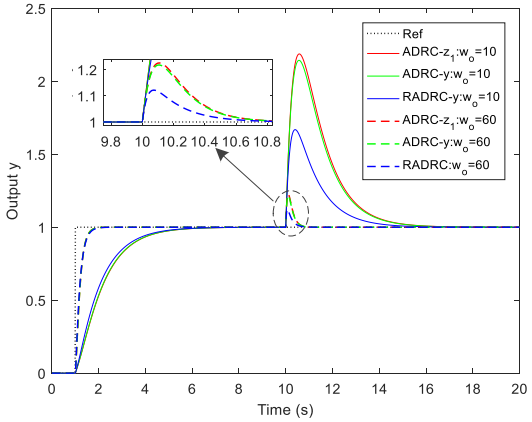

Fig. 2 The step-response and disturbed process of the compared controllers

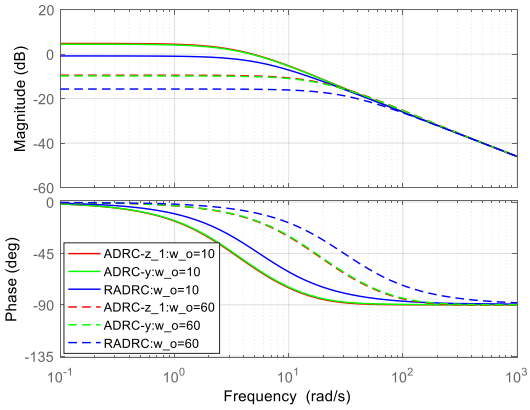

Fig. 3 The inner loop bode diagram for the compared controllers

Table 2. The Control Parameters under Two Different Observer Bandwidths

	ω_o	k_p	b_0
Parameters Set 1	10	1	10
Parameters Set 2	60	5	10

3.2 Discrete ADRC with variable sampling technique

The variable sampling rate based ADRC for marine engine speed control is introduced here briefly. More details can refer to (Wang et al., 2019b). The fuel injection quantity for individual cylinder W_f^i is set to be the controlled input. Reconstructing (6) gets

$$\frac{d}{dt}n_e = \frac{30}{\pi J_e}\left(\frac{1}{W_f^i}M_{ig}W_f^i - M_{total}\right), \tag{14}$$

Given $\frac{30}{\pi J_e W_f^i}M_{ig} = b_0 + \Delta b$, b_0 being an estimate of $\frac{30}{\pi J_e W_f^i}M_{ind}$, (17) can be rewritten as

$$\frac{d}{dt}n_e = b_0 W_f^i + f(t), \tag{15}$$

where $f(t) = \Delta b W_f^i - \frac{30}{\pi J_e} M_{total}$ is regarded as the total disturbance.

If choose state variables as $x_1 = n_e$, $x_2 = f(t)$, control input $u = W_f^i$, and consider the CA based control, which means that the output $y(t_k)$ and the control input $u(t_k)$ can only be updated once for each cylinder per working cycle, hence, the extended state space model for (15) can be given as

$$\begin{cases} \dot{\boldsymbol{x}}(t) = \boldsymbol{A}\boldsymbol{x}(t) + \boldsymbol{B}u(t_k) + \boldsymbol{E}\dot{f}(t) \\ y(t_k) = \boldsymbol{C}\boldsymbol{x}(t_k), t \in [t_k, t_k + \Delta t_{k,n_e}), k = 0,1, \ldots \end{cases}, \quad (16)$$

where $\boldsymbol{A} = \begin{bmatrix} 0 & 1 \\ 0 & 0 \end{bmatrix}$, $\boldsymbol{B} = \begin{bmatrix} b_0 \\ 0 \end{bmatrix}$, $\boldsymbol{C} = [1,0]$, $\boldsymbol{E} = \begin{bmatrix} 0 \\ 1 \end{bmatrix}$, $\boldsymbol{x} = \begin{bmatrix} n_e \\ f \end{bmatrix}$, t_k is the real time when sampling instance k comes, $\Delta t_{k,n_e}$ is the sampling interval that varies with mean engine speed, and can be calculated by (17),

$$\Delta t_{k,n_e} = \frac{\pi \cdot n_{e,k}}{30 \Delta \theta_{firing}}, \quad (17)$$

where $n_{e,k}$ is the average engine speed at the sampling point k, $\Delta\theta_{firing}$ is the firing interval of the engine.

Refer to (Miklosovic et al., 2006), the discrete-time ESO with variable sampling rate can be written as follow

$$\begin{cases} \boldsymbol{z}(k+1) = \boldsymbol{\Phi}\left(\Delta t_{k,n_e}\right)\boldsymbol{z}(k) + \left[\boldsymbol{\Gamma}\left(\Delta t_{k,\varphi}\right), \boldsymbol{L}_c\right]\boldsymbol{U}(k) \\ \qquad\qquad + \boldsymbol{O}\left(\Delta t_{k,n_e}{}^2\right) \\ \hat{y}(k) = \boldsymbol{C}\hat{\boldsymbol{x}}(k), \end{cases}, (18)$$

where $\boldsymbol{z}(k) = \boldsymbol{z}(t)|_{t\in[t_k, t_k+\Delta t_{k,n_e})}$, $\boldsymbol{\Phi}\left(\Delta t_{k,n_e}\right) = \boldsymbol{A_d}(\Delta t_{k,n_e}) - \boldsymbol{L}_c\boldsymbol{C}\boldsymbol{A_d}(\Delta t_{k,n_e})$, $\boldsymbol{\Gamma}\left(\Delta t_{k,n_e}\right) = \boldsymbol{B_d}\left(\Delta t_{k,n_e}\right) - \boldsymbol{L}_c(\Delta t_{k,n_e})\boldsymbol{C}\boldsymbol{B_d}(\Delta t_{k,n_e})$, $\boldsymbol{L}_c = \begin{bmatrix} l_1 \\ l_2 \end{bmatrix}$, $\boldsymbol{A_d}\left(\Delta t_{k,n_e}\right) = \begin{bmatrix} 1 & \Delta t_{k,n_e} \\ 0 & 1 \end{bmatrix}$, $\boldsymbol{B_d}\left(\Delta t_{k,n_e}\right) = \begin{bmatrix} b_0 \Delta t_{k,n_e} \\ 0 \end{bmatrix}$, $\boldsymbol{z} = \begin{bmatrix} z_1 \\ z_2 \end{bmatrix}$, $\boldsymbol{U}(k) = \begin{bmatrix} u(k) \\ y(k) \end{bmatrix}$.

The control law can be given as

$$u(k) = \frac{\omega_c{}'\left(r(k) - z_1(k)\right) - z_2(k)}{b_0}, \quad (19)$$

or

$$u(k) = \frac{\omega_c{}'\left(r(k) - y(k)\right) - y(k)}{b_0}. \quad (20)$$

Due to the varying of sampling interval, the control parameters are designed to be variable with sampling step, they are

$$\boldsymbol{L}_c\left(\Delta t_{k,n_e}\right) = \begin{bmatrix} 1 - \beta'^2 \\ \dfrac{(1-\beta')^2}{\Delta t_{k,n_e}} \end{bmatrix}, \quad (21)$$

$$\beta'\left(\Delta t_{k,n_e}\right) = e^{-\omega_o{}' \Delta t_{k,n_e}}, \quad (22)$$

where $\omega_o{}' = \alpha\omega_{o,n_{e0}}$, $\omega_c{}' = \alpha\omega_{c,n_{e0}}$, $\omega_{o,n_{e0}} = (3\sim10)\omega_{c,n_{e0}}$, $\omega_{c,n_{e0}} = (4\sim10)/T_{settle,n_{e0}}$, $\alpha = n_e(k)/n_{e0}$, α is a coefficient changing with engine speed, n_{e0} is the nominal speed for rating condition, $T_{settle,n_{e0}}$ is the desired settling time under nominal speed, $\omega_{o,n_{e0}}$ and $\omega_{c,n_{e0}}$ are the observer bandwidth and control bandwidth under the nominal speed n_{e0}, respectively, $\omega_o{}'$ and $\omega_c{}'$ mean the modifed observer and control bandwidth, respectively.

Remark 2. The settling time $T_{settle,n_{e0}}$ should be different under different engine speed. If adopt a single settling time to design the parameters in ESO and control law, the control performance for the whole operation conditions cannot be guaranteed. If do not consider the parameters design in (21) and (22), extra calibration for different speed stages should be considered for proper control performance during the whole speed ranges, which has been proved in (Wang et al., 2019a). This trait is related to the inherent property of the diesel engine.

3.3 Discrete RADRC with variable sampling technique

As shown above that the sampling interval under a certain engine speed is limited. Hence, the performance of ESO cannot be further improved by increasing observer bandwidth. In addition, the larger the observer bandwidth, the easier the control system becomes unstable. Under such condition, RADRC is a better choice. Considering (16), the RESO can be given as following with the variable sampling interval $\Delta t_{k,n_e}$,

$$\begin{cases} v(k+1) = v(k) - l\Delta t_{k,n_e}(b_0 u(k) + (v(k) + l x_1(k))) \\ z_2(k) = v(k) + l x_1(k) \end{cases}, \quad (23)$$

where l is the observer bandwidth of the RESO.

The control law for RADRC can be given as

$$u(k) = \frac{\omega_c{}'\left(r(k) - y(k)\right) - z_2(k)}{b_0}, \quad (24)$$

Remark 3. The observer bandwidth l in RESO can be designed to be smaller than $\omega_{o,n_{e0}}$, making it can compromise to a wide engine speed range, and no need to vary with the engine speed. But the control bandwidth $\omega_c{}'$ in control law (24) for RADRC is designed to be the same as in the general ADRC.

4. SIMULATIONS AND ANALYSIS

In order to verify the proposed control scheme, the simulations are given based on a general engine control hard-in-loop (HIL) test platform (Wang et al., 2019b).

The control parameters for the general ADRC and RADRC are given in Table 3.

Table 3. The Control Parameters

Controller	Control bandwidth	Observer bandwidth	b_0
ADRC-z1 and ADRC-y	$\omega_c{}' = \alpha\omega_{c,n_{e0}} = 12\alpha$; $\alpha = n_e/n_{e0} = n_e/1800$	$\omega_o{}' = \alpha\omega_{o,n_{e0}} = 60\alpha$	25
RADRC	$\omega_c{}' = \alpha\omega_{c,n_{e0}} = 12\alpha$ $\alpha = n_e/n_{e0} = n_e/1800$	$l = 40$	25

Note: $n_{e0} = 1800$ means the parameters are adjusted around the rated condition, i.e., full load at 1800 rpm.

Figure 4 illustrates the speed responses for the compared controllers during the set-point tracking processes and the sudden load changing processes. At 13s, the external torque is removed totally and added again at 15s. The corresponding control signal and estimated total disturbance z_2 are given in Fig. 5 and Fig. 6, respectively.

It can be seen from Fig. 4 that, for the speed tracking processes, the three controllers obtain the similar settling time and without significant overshoot. ADRC-y gives slower set-point tracking speed. This because $z_1(k)$ has a difference with

$x_1(k)$, i.e. y, then the absolute error $|r(k) - y(k)|$ in control law (20) for ADRC-y is smaller than the absolute error $|r(k) - z_1(k)|$ in control law (19) for ADRC-z1, and the same time, the disturbance estimation for ADRC-z1 and ADRC-y are almost the same during the set-point tracking processes (see Fig. 6). However, during the sudden load changing conditions, the speed deviations in RADRC are the smallest (see Fig.4, Zoom4), followed by ADRC-y and then ADRC-z1, which indicates that, for marine engine speed control, the order-reduction can improve the anti-interference ability of ADRC, and using the system output y in control law can significantly reduce the speed deviation during the load disturbance. To compare the controllers more reasonable, the performance criteria in integral absolute error (IAE) of the system output, the total variation (TV) of the control input, and the speed deviation during the sudden load varying conditions are provided in Table 4. The IAE and TV indexes can refer to (Skogestad, 2003).

In terms of IAE, single set of parameters in RADRC can keep a good compromise during the high and low speed zones. In ADRC-z1 and ADRC-y, observer bandwidth near the rated condition (1800 rpm, full load) is designed to be 60, which can guarantee a proper speed deviation under sudden load change (as shown in Fig. 4, Zoom4). If the observer bandwidth is set bigger, the steady-state speed fluctuation would be worse, especially, the IAE in ADRC-z1 and ADRC-y would be bigger during the low-speed range. It implies that, for general ADRC, the contradiction between the steady-state performance under different engine speed region and the disturbance rejection requirement during the sudden load changing condition is hard to get a proper compromise. It is necessary to change the observer bandwidth in ADRC for different engine speed. Whereas, in RADRC, such contradiction is weaker because the observer bandwidth can be designed to be relatively smaller.

For TV criterion, its values in RADRC are apparently larger than that in ADRC. This phenomenon should be understood in two aspects, on the one hand, compared with ESO, the RESO estimates the noise torque disturbance faster under steady-state then compensates it in the control signal with a bigger fluctuation. This can be proved by the relative smaller IAE values in RADRC.

Table 4. The Performance indexes for the Controllers

Controller	IAE	TV	Speed deviation
ADRC-z1	1.64^1, 2.12^2, 3.59^3	11.82^1, 44.52^2, 149.91^3	137.0^a, 130.7^b
ADRC-y	1.46^1, 2.68^2, 3.19^3	10.41^1, 52.02^2, 131.23^3	123.6^a, 119.0^b
RADRC	1.47^1, 2.67^2, 3.16^3	21.14^1, 76.19^2, 169.87^3	111.2^a, 107.0^b

Note: ^{1,2,3} means the steady-state processes during the time 3s to 5s, 8s to 10s, 11s to 13s, respectively, the corresponding reference speed is 800rpm, 1300rpm, and 1800rpm. $^{a,\ b}$ denotes the sudden unloading and sudden loading process, respectively.

On the other hand, the inherent engine speed fluctuation caused by discrete indicated torque production and imbalance powering in individual cylinder is treated as caused by disturbance for ADRC and RADRC. As RADRC has faster disturbance estimation, hence, RADRC generates more compensation in control signal for such inherent engine speed fluctuation (see in Fig. 6), which means the control signal changes more in RADRC, resulting in more aggressive control input. For a six-cylinder diesel engine, ignore the in-cylinder gas force, during steady-state the frequency of engine speed fluctuation, ω_f, is related to firing interval, which can be calculated by

$$\omega_f = 2\pi \frac{n_e}{60} = \frac{\pi n_e}{30}. \tag{25}$$

For instance, when reference speed is 1800 rpm, the engine speed fluctuation frequency is around 1130 rad/s. Because the bode diagram in Fig. 3 is obtained around 1800 rpm, we can know that the inner loop of RADRC attenuates more the amplitude of the input disturbance signal, making more oscillation in the estimated total disturbance z_2 then causing the control signal with more oscillation.

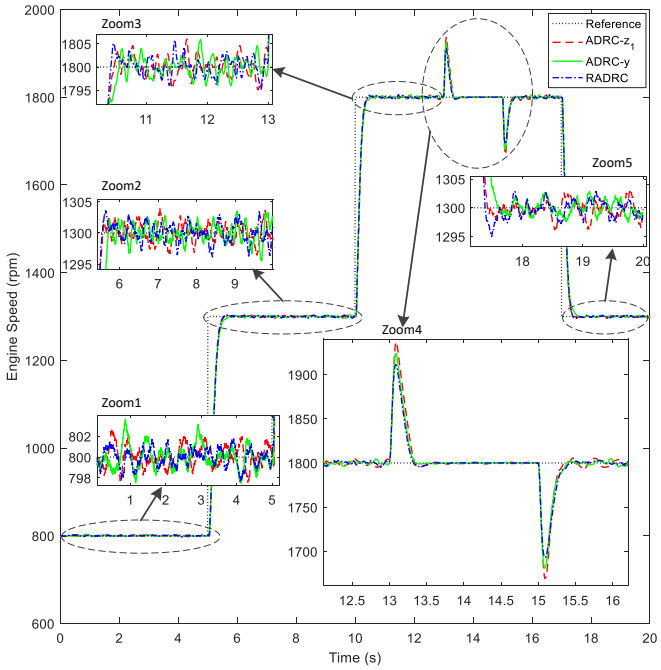

Fig. 4 The speed responses for the compared controllers

But as the TV values for RADRC (showing in Table 2) are not extremely larger than that in ADRC, hence, it is still acceptable.

As for the speed deviation during the sudden load change conditions, the RADRC performs its superiority. In average, the speed deviation in RADRC is around 10% and 18% less than in ADRC-y and ADRC-z1, respectively. Note that, it is of importance that the engine speed can recover faster and with less speed deviation during the sudden load change conditions for marine diesel engine. It directly affects the voyage safety of the ship and the safety of the marine diesel engine (Lynch et al., 2006). From this perspective, the RADRC is the most preferred controller for marine engine speed control.

5. CONCLUSIONS

In this study, the discrete RADRC with variable sampling rate technique is designed for marine engine speed control. From the view of frequency domain analysis, the benefit of RADRC is analysed by using the transfer function between input disturbance and system output. This is different from some previous works. The experiment on the HIL system

demonstrates that the RADRC has significant advantages during the load torque sudden changing processes. In terms of IAE criterion under steady-state, overall, RADRC also has the best performance during different reference speed which ranges from low-speed to high-speed. The only issue should be noted in RADRC is the TV index for control signal, however, it is still in an acceptable region. This study indicates that the RADRC approach is a promising choice for marine engine speed control, with which the calibration for marine engine speed controller can be reduced significantly.

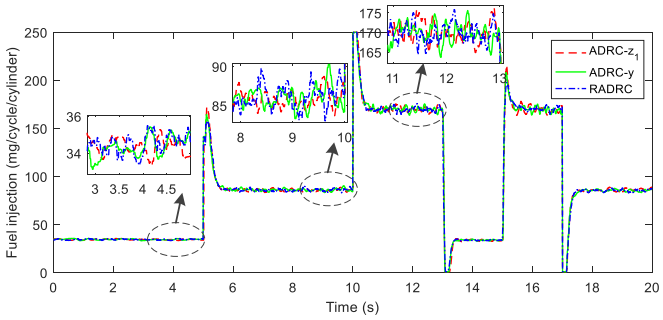

Fig. 5 The control signal for the compared controllers

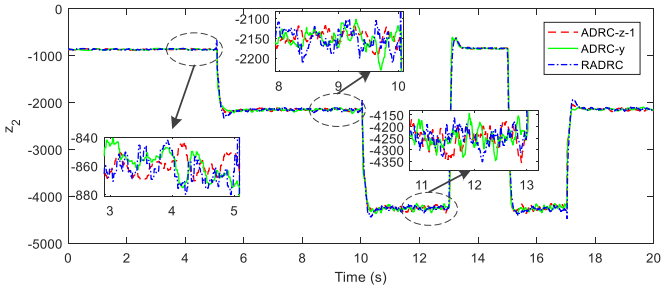

Fig. 6 The estimated total disturbance z_2 for the compared controllers

REFERENCES

BROOMHEAD, T., MANZIE, C., HIELD, P., SHEKHAR, R. & BREAR, M. 2017. Economic model predictive control and applications for diesel generators. *IEEE Transactions on Control Systems Technology,* 25**,** 388-400.

CHEN, S., XUE, W. & HUANG, Y. 2019. Analytical design of active disturbance rejection control for nonlinear uncertain systems with delay. *Control Engineering Practice,* 84**,** 323-336.

GAO, Z. Scaling and bandwidth-parameterization based controller tuning. Proceedings of the American Control Conference, 2003. 4989-4996.

HUANG, Y. & XUE, W. 2014. Active disturbance rejection control: Methodology and theoretical analysis. *ISA Transactions,* 53**,** 963-976.

JAMMOUSSI, H., FRANCHEK, M., GRIGORIADIS, K. & BOOKS, M. 2014. Closed-loop system identification based on data correlation. *Journal of Dynamic Systems Measurement and Control-Transactions of the ASME,* 136.

LI, X., AHMED, Q. & RIZZONI, G. 2017. Nonlinear robust control of marine diesel engine. *Journal of Marine Engineering & Technology,* 16**,** 1-10.

LYNCH, C., HAGRAS, H. & CALLAGHAN, V. 2006. Using uncertainty bounds in the design of an embedded real-time type-2 neuro-fuzzy speed controller for marine diesel engines. IEEE International Conference on Fuzzy Systems, Jul 16-21 2006 Vancouver, Canada. 1446-1453.

MEMERING, D. W. & MECKL, P. H. 2002. Comparison of adaptive control techniques applied to diesel engine idle speed regulation. *Journal of Dynamic Systems Measurement and Control-Transactions of the ASME,* 124**,** 682-688.

MIKLOSOVIC, R., RADKE, A., GAO, Z. 2006. Discrete implementation and generalization of the extended state observer. American Control Conference, Jun 14-16 2006 Minneapolis, MN. 2209-2215.

PAPALAMBROU, G. & KYRTATOS, N. P. 2006. H_∞ Robust control of marine diesel engine equipped with power-take-in system. *IFAC Proceedings Volumes,* 39**,** 591-596.

SHAO, X. & WANG, H. 2015. Back-stepping active disturbance rejection control design for integrated missile guidance and control system via reduced-order ESO. *ISA Transactions,* 57**,** 10-22.

SKOGESTAD, S. 2003. Simple analytic rules for model reduction and PID controller tuning. *Journal of Process Control,* 13**,** 291-309.

TATSUMI, J., GAO, Z. 2013. On the enhanced ADRC design with a low observer bandwidth. 32nd Chinese Control Conference (CCC), Jul 26-28 2013 Xian, China. 297-302.

WANG, R., LI, X., AHMED, Q., ZHANG, J., LIU, Y. & MA, X. 2019a. Crank-angle based active disturbance rejection control for a marine diesel engine. 2019 American Control Conference (ACC), 10-12 July 2019. 18-23.

WANG, R., LI, X., LIU, Y., AHEMD, Q., YANG, Y., FENG, C. & MA, X. 2019b. Variable sampling rate based active disturbance control for a marine diesel engine. *Electronics,* 8.

WANG, R., LI, X., ZHANG, J., ZHANG, J., LI, W., LIU, Y., FU, W. & MA, X. 2018a. Speed control for a marine diesel engine based on the combined linear-nonlinear active disturbance rejection control. *Mathematical Problems in Engineering*.

WANG, R. Z., LI, X. M., LIU, Y. F., FU, W. J., LIU, S. & MA, X. Z. 2018b. Multiple model predictive functional control for marine diesel engine. *Mathematical Problems in Engineering*.

WEIGANG, P., HAIRONG, X., YAOZHEN, H., CHANGSHUN, W. & GUIYONG, Y. Nonlinear active disturbance rejection controller research of main engine for ship. 2010 8th World Congress on Intelligent Control and Automation, 7-9 July 2010. 4978-4981.

YANG, R., SUN, M. & CHEN, Z. 2011. Active disturbance rejection control on first-order plant. *Journal of Systems Engineering and Electronics,* 22**,** 95-102.

YUAN, Y., ZHANG, M., CHEN, Y. & MAO, X. 2018. Multi-sliding surface control for the speed regulation system of ship diesel engines. *Transactions of the Institute of Measurement and Control,* 40**,** 22-34.